



Analysis of Seismic Vulnerability Index Based on Microtremor Investigation (Case Study of Majangtengah Village, Dampit, Malang Regency)

Siti Rohmah¹, Adi Susilo¹(✉), Didik Yudianto¹, Farizky Hisyam¹, Eko Andi Suryo², and Sarjiyana³

¹ Geophysical Engineering, Faculty of Mathematics and Science, Brawijaya University, Malang, Indonesia

adisusilo@ub.ac.id

² Civil Engineering Department, Faculty of Engineering, Brawijaya University, Malang, Indonesia

³ Department of Mechanical Engineering, Politeknik Negeri Malang, Malang, Indonesia

Abstract. Some of the damage caused by earthquakes is not always caused by the strength of the earthquake or the distance from the epicenter of the earthquake to the affected buildings but is also influenced by local geological conditions. Majangtengah Village, Dampit District, Malang Regency is one of the areas that experienced considerable damage due to the earthquake in southern East Java on April 10, 2021. One of the geophysical surveys used to determine the potential for local site effect hazards is the microtremor survey. This study aims to determine the level of soil vulnerability based on the value of dominant frequency (f_0), amplification (A_0), and seismic vulnerability index (K_g) using HVSR analysis. Microtremor data measurements include 9 points with a recording duration of 45 min. The results of microtremor data analysis obtained dominant frequency values (f_0) between 2.42–4.33 Hz, amplification values (A_0) between 2.78–8.19, and seismic vulnerability index values (K_g) between 3.19–20.11 cm/s^2 . This condition illustrates that the research area is unstable because it has a high vulnerability index value.

Keywords: Microtremor · Dominant frequency · Amplification · Seismic Vulnerability Index

1 Introduction

A disaster is an event that threatens and disrupts people's lives caused by natural and non-natural factors. The impact of disasters can result in casualties, environmental damage, loss of property, and psychological impacts [1]. Malang Regency is one of the areas that often feel the impact when tectonic earthquakes occur. This is because the tectonic dynamics in the southern part of the Malang region are dominated by the movement of the India-Australia plate which moves north to collide with the relatively still Eurasian plate [2].

© The Author(s) 2023

E. Susanti et al. (Eds.): ICGT 2022, AER 221, pp. 149–158, 2023.

https://doi.org/10.2991/978-94-6463-148-7_16

The research area is administratively included in the Malang Regency area. Based on the geological map, the districts of Malang and Lumajang are included in the Turen Sheet. It is located between the coordinates $112^{\circ}30' - 113^{\circ}00'E$ and $8^{\circ}00' - 8^{\circ}30' LS$. The tectonic influence of the Turen Sheet is characterized by the presence of faults, slopes, and calderas. Seismic activity in the Malang area is not only caused by the subduction zone located in the south of Java Island but also caused by fault activity, both locally and regionally [3]. Recent studies have revealed the existence of a new earthquake source that spans 300 km from the south of Semarang, Central Java, to East Java. The source of the latest earthquake comes from the Kendeng Fault [4].

Several sub-districts that are prone to tectonic earthquakes in Malang Regency include Gedangan, Sumbermanjing Wetan, Dampit, Tirtoyudo, and Ampelgading Districts. Based on the geological map and the results of the interpretation of the gravity data, it shows that there are results of the corresponding local fault trajectories/locations. The carrying capacity of the rocks in these pathways is relatively lower than that of the surroundings so these pathways are unstable [5].

One of the earthquakes that caused considerable damage in Malang Regency was an earthquake that occurred on 10th April 2021 at 14:00 WIB with a magnitude of 6.1 SR the impact of this earthquake reached the maximum intensity scale of V-VI MMI so it has the potential to be destructive. The earthquake resulted in 9 deaths in Malang and Lumajang regencies, and 121 people were injured in Malang and Blitar regencies. In addition, as many as 2,491 buildings were severely damaged, 5,038 buildings were moderately damaged, 6,472 buildings were lightly damaged, and 649 public facilities buildings suffered general damage. Locations of damage to buildings are spread out in the Regencies of Malang, Malang City, Lumajang, Blitar, Trenggalek, Batu, Nganjuk, and Pacitan.

This research was conducted in areas that have been affected by earthquake damage. Several buildings in this area suffered heavy damage including public facilities (Mousque). It aims to determine the characteristics of soil sediments. The characteristics of soil sediments can be analyzed based on the value of dominant frequency (f_0), amplification (A_0), and seismic vulnerability index (K_g). Geological conditions and soil types can affect the level of damage caused by an earthquake. To determine the potential danger of local site effects (geological conditions) in this area, an in-depth study is needed through an initial survey, namely microtremor measurements on a local scale, namely in Majangtengah Village, Dampit District, Malang Regency.

Microtremor surveys have been widely applied in various studies with wide area coverage, including (1) analyzing ground motion values (PGA), *Peak Spectral Acceleration (PSA)*, and *shake maps*, (2) making microzonation maps to study seismic susceptibility and soil dynamic characteristics, (3) analyzing quaternary sediments and seismic susceptibility zones and (4) knowing the relationship between seismic susceptibility and the physical vulnerability of buildings in areas that experienced the worst damage due to earthquakes. This method is considered cheaper and easier to implement so that disaster mitigation efforts and mapping of disaster-prone areas can be carried out quickly and accurately. This can help minimize the impact of damage and casualties due to earthquakes.

2 Research Method

Microtremor is a small and continuous ground vibration that comes from two main sources, namely natural and human activities [6]. Microtremors have a higher frequency than earthquakes (>0.1 s or generally between 0.05–2 s) and long-term microtremors can reach 5 s, while the amplitude ranges from 0.1 to 2.0 microns [7].

Microtremor data can be used to determine the dynamic characteristics of the soil surface layer. One of the methods used in microtremor analysis is the *Horizontal to Vertical Spectrum Ratio (HVSr)* method.

The *HVSr* method was first introduced by Nogosi and Igarashi (1971) [8], then modified and developed by Yutaka Nakamura [9]. This method uses three-component microtremor vibration recording data (N-S, E-W, and Z components). The formulation of the *HVSr* equation is as in Eq. 1 [9].

$$T_{\frac{H}{V}}(\omega) = \frac{S_{NS}(\omega) + S_{EW}(\omega)/2}{S_V(\omega)} \quad (1)$$

The location for microtremor data collection was carried out in Majangtengah Village, Dampit District, Malang Regency. This area is located around the Wonosari fault (*Tmwl*) with the Wuni formation dominated by lava breccias, lava breccias, tuff breccias, and sandy tuffs. Data collection was carried out based on SESAME rules [10]. Data collection was shown in Fig. 1.

Data collection was carried out by the BMKG Class II Pasuruan team using the *TDL-303S Digital Portable Seismograph* with 9 points. Data collection locations are at $08^{\circ}11'40.04''$ - $08^{\circ}11'35.01''$ LS and $112^{\circ}43'03.81''$ - $112^{\circ}42'50.48''$ BT. Duration of microtremor recording for 45 min at each point with a sampling frequency of 100 Hz and a target frequency of 0–20.

Microtremor data processing using *geopsy* software with the *HVSr* method. In the filtering process, the signal is taken with a bandpass of 0.5–25 Hz, so that the signal taken is under the character of the microtremor signal, namely a low-frequency signal. Signal selection (*windowing signal*) is performed to separate the tremor signal from the transient event. The frequency calculation process uses *Fast Fourier Transform (FFT)* on each component. The principle is to approach each signal so that it produces an



Fig. 1. Location of Measurement Points

amplitude. The amplitude value represents the signal associated with the frequency. *The Fast Fourier transform (FFT)* is defined as in Eq. 2.

$$x(\omega) = \int_{-\infty}^{\infty} x(t)e^{-i\omega t} dt \quad (2)$$

$$\int_{-\infty}^{\infty} x(t) \cos(\omega t) dt - i \int_{-\infty}^{\infty} x(t) \sin(\omega t) dt$$

The obtained *HVSR* curve produces the dominant frequency value (f_0), and amplification value (A_0) from each measurement point. The dominant frequency value (f_0) is used to estimate the thickness of the layer, the dominant period value (T_0) is used to estimate the rock hardness level, and the soil amplification value (A_0) provides an overview of changes (magnification) of the acceleration of soil movement from the bedrock to the surface [11]. Another parameter used is the seismic vulnerability index (K_g). The calculation of the seismic vulnerability index (K_g) based on the comparison of the square of the amplification value (A_0) with the dominant frequency (f_0) in the study area is written in Eq. 3 [11].

$$K_g = \frac{A_m^2}{f_0} \quad (3)$$

3 Discussion

Therefore, disaster mitigation efforts are important to minimize the impact of damage and casualties. This can be done by knowing the causes of earthquakes and zones that are highly vulnerable to zones that are relatively safe from earthquake hazards.

The shape of the resulting *HVSR* curve varies at each measurement point. This is caused by subsurface geological conditions and the process of recording microtremor data. The characteristics of the *HVSR* curve are shown by the curve pattern formed, this curve pattern is used for local geological characterization. Based on the results of data processing, the research location produces two types of curve topology including a curve with one peak (*clear peak*) and a wide peak curve (*broadband*).

Figure 2 (a) shows the topology of the curve with one clear peak. The curve shows that there is impedance contact at a certain depth so that the wave experiences amplification (strengthening). While Fig. 2 (b) shows the topology of the curve with a broad peak (*broadband*). The shape of the curve with wide peaks may be related to local geological conditions, this is related to the presence of sloping basins (*bedrock*) or variations in bedrock sedimentary structures. Among the causes of variations in the shape of the *HVSR* curve are variations in impedance contrast, layer compactness, rock hardness, subsurface geology, and others.

3.1 Microzonation of Dominant Frequency Value (f_0)

The dominant frequency is a frequency value that indicates the type and characteristics of rock layers in the region. This value is generated from the analysis of the *HVSR*

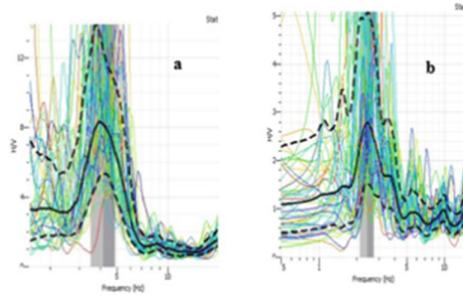


Fig. 2. (a) Topology of a single peak (*clear peak*) HVSR curve (b) Topology of a wide peak (*broadband* HVSR curve)

method. The map of the distribution of dominant frequency values at the study locations is shown in (Fig. 3). The dominant frequency value (f_0) ranges from 2.42 Hz–4.33 Hz.

Based on the soil classification by Kanai and Omote-Nakajima [12], Fig. 3 shows that the study area has varying soil frequency values. Low-frequency values are indicated by the blue anomaly, namely at points WR1, WR2, WR3, WR4, WR5, WR7, and WR8. This area can be said to be a low zone with dominant frequencies ranging from 2.42 Hz–2.44 Hz. The low zone may have a fairly thick sediment thickness (10–30 m). The moderate zone has dominant frequency values ranging from 4 Hz–10 Hz [12], (Fig. 3) the moderate zone is indicated by an anomaly in red with a dominant frequency value of 4.33 Hz. The moderate zone has sediment thickness between 5–10 m.

The dominant period value (T_0) is related to the depth of the soft sediment layer. A high dominant period (T_0) in an area indicates thick soft sediments that tend to experience high reinforcement so that they are susceptible to damage and vice versa, a low dominant period indicates thin soft sediments [13].

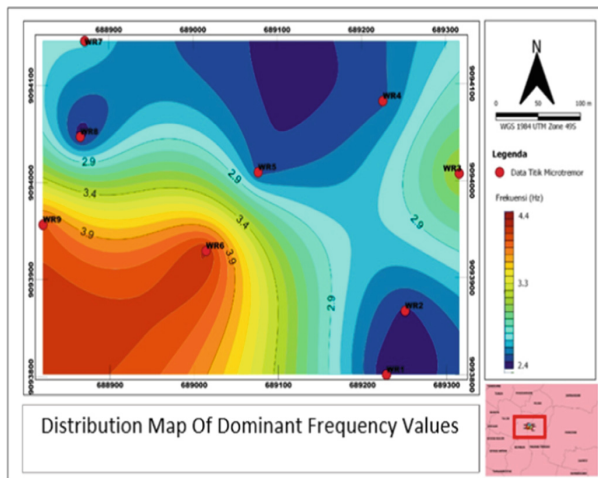


Fig. 3. Map of distribution of dominant frequency values (f_0) at measurement points

Table 1. Classification of frequency zones in the study area

Point	(f_0)	(T_0)	Class	Character
WR1	2.42	0.41	C/IV	Very Soft
WR2	2.48	0.40	B/III	Soft
WR3	3.34	0.30	B/III	Soft
WR4	2.58	0.39	B/III	Soft
WR5	2.57	0.39	B/III	Soft
WR6	4.33	0.23	A/II	Medium
WR7	2.82	0.35	B/III	Soft
WR8	2.44	0.41	C/IV	Very Soft
WR9	4.13	0.24	A/II	Medium

Based on the dominant period (T_0) value, the research area is in various zones: zone II, zone III, and zone IV. Zone II, namely at points (WR6 and WR9) is indicated by the dominant period (T_0) between 0.15–0.25 s, this area is categorized as a medium soil type with alluvial rock consisting of gravel sand, hard clay, clay, and loam. While zone III dominates this area, namely at points (WR2, WR3, WR4, WR5, and WR7) which are indicated by the dominant period (T_0) values between 0.25–0.40 s, this area is categorized as a soft soil type with almost the same alluvial rock. With the constituent rocks in zone two, but in this zone, there are bluff formations. Zone IV, namely at points (WR1 and WR8) indicated by a dominant period value (T_0) > 0.40 s, this area is categorized as a very soft soil type with alluvial rock formed from deltaic sedimentation, topsoil, silt, humus, deltaic deposits or silt. The table of soil classification in the study area is shown in Table 1.

3.2 Microzonation of Soil Amplification Value (A_0)

The amplification factor of the soil spectrum (A_0) is the peak value of the HVSR curve which describes the physical properties of the hardness and softness of the sediment. The magnitude of the amplification can be estimated from the impedance contrast between bedrock and surface sediments [14].

The distribution of soil amplification values in the study area is shown in Fig. 4. The soil amplification values ranged from 2.78–8.19. Based on the classification by Setiawan [15], the soil amplification factor values are divided into 4 zones, namely: low amplification zone ($A_g < 3$), medium amplification zone ($3 \leq A_g < 6$), high amplification zone ($6 \leq A_g < 9$), and very high amplification zone ($A_g \geq 9$).

Based on the distribution of the soil amplification value (A_0), the research area is known to have varying values. Soil classification based on the amplification value (A_0) can be divided into 4 zones, namely: low amplification zone ($A_g < 3$), medium amplification zone ($3 \leq A_g < 6$), high amplification zone ($6 \leq A_g < 9$), and very amplification zone height ($A_g \geq 9$).

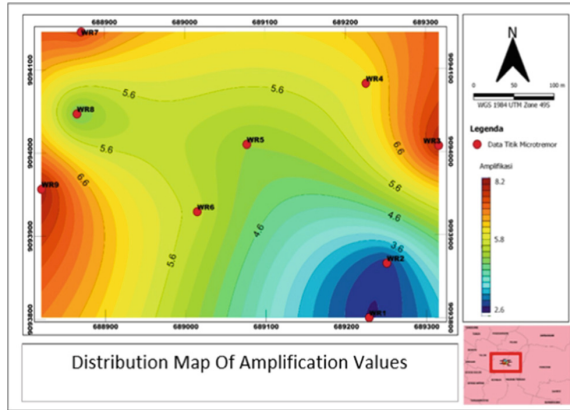


Fig. 4. Distribution of soil amplification values (A_0) at measurement points

The research area which is included in the low zone ($A_g < 3$) includes points (WR1 and WR2) with soil amplification values of 2.74 to 2.84, this zone is indicated by an anomaly in blue. While the area included in the medium amplification zone ($3 \leq A_g < 6$) includes points (WR5, WR6, and WR8) with soil amplification values of 4.67 to 5.50, this zone is indicated by an anomaly in yellow. The research area which is included in the high amplification zone ($6 \leq A_g < 9$) includes points (WR3, WR4, WR7, and WR9) with soil amplification values of 6.08 to 8.19, these zones are indicated by the red anomaly. The classification of soil in the study area is shown in Table 2.

The soil amplification value (A_o) is related to the amplification of waves or the response of the surface layer to shocks [16]. If the amplification factor value of the soil spectrum is large, the sediment in the area is getting softer, and vice versa if the amplification factor value of the soil spectrum is low, the sediment layer is harder. So it can be concluded that areas in the high amplification zone allow for the potential for

Table 2. Soil Classification Based on Amplification Value (A_0)

Point	Amplification (A_0)	Zone	Description
WR1	2.78	1	Low Amplification
WR2	2.84	1	Low Amplification
WR3	8.03	3	High Amplification
WR4	6.08	3	High Amplification
WR5	5.01	2	Medium Amplification
WR6	5.50	2	Medium Amplification
WR7	7.53	3	High Amplification
WR8	4.67	2	Medium Amplification
WR9	8.19	3	High Amplification

strong ground movement and damage to buildings in the area is also greater if exposed to earthquake shocks.

The soil amplification factor (A_0) gives an idea of the change (magnification) of the acceleration of ground motion from bedrock to the surface caused by differences in shear wave velocity (V_s) in the bedrock and soil layer (sediment). The lower the base wave velocity (V_s) will cause a decrease in the value of the shear modulus (G_s) and the damping factor (μ), so it can be concluded that the greater the amplification value, the greater the acceleration of ground motion on the surface.

3.3 Microzonation of Seismic Vulnerability Index (K_g)

The seismic vulnerability index (K_g) is an index that describes the level of vulnerability of the surface soil layer to deformation during an earthquake. The value of the seismic vulnerability index is influenced by the value of the soil amplification factor and the dominant period of the soil. The value of the seismic vulnerability index (K_g) is used to estimate an area that is prone to ground movement, this value also depends on soil conditions.

The distribution of seismic vulnerability index values (K_g) in the study area is shown in Fig. 5. Seismic vulnerability index values (K_g) ranged from 3.19 cm/s^2 –20.11 cm/s^2 .

Based on the figure, relatively high seismic vulnerability index (K_g) values include points (WR3, WR4, WR5, WR7, WR8, and WR9) which are indicated by yellow and red anomalies. High seismic susceptibility index (K_g) values are obtained in areas with high amplification values (A_0) and low dominant frequency values (f_0). This shows that there is a relationship between the thickness of the soil layers with high compactness.

The relatively low value of the seismic vulnerability index (K_g) includes points (WR1, WR2, and WR6) which are indicated by blue anomalies. Low seismic vulnerability index (K_g) values are obtained in areas with low amplification values (A_0) and high dominant frequency values (f_0). The area has a low impedance contrast with a thin layer of sediment, this area is generally located in hilly areas. Research [17] explained

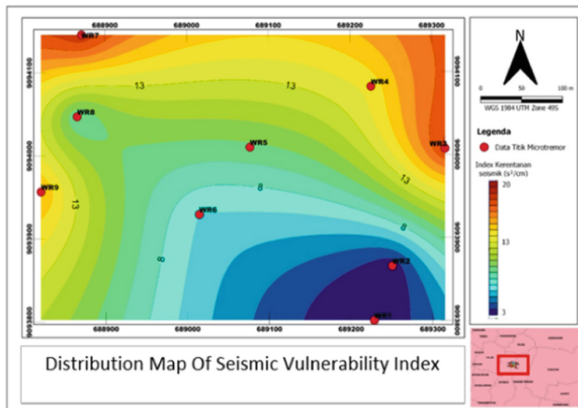


Fig. 5. Distribution of Seismic Vulnerability Index Values (K_g) at measurement points

that the damage caused by an earthquake is proportional to the seismic vulnerability index value.

In the research area, it is known that at points (WR1, WR2, WR4, and WR5) experienced a considerable impact such as heavy damage to residents' houses, mosques, and several other public facilities.

4 Conclusion

The results of the microtremor survey in Majangtengah Village, Dampit District, Malang Regency show that the dominant frequency value (f_0) ranges from 2.42 Hz–4.33 Hz, the soil amplification value (A_0) ranges from 2.28–8.29, and the seismic vulnerability index value (K_g) ranges from 3.19 cm/s²–20.11 cm/s². This value illustrates that the study area is unstable and quite vulnerable because it has a relatively low dominant frequency value (f_0), as well as a relatively high soil amplification value (A_0) and seismic vulnerability index (K_g). It is characterized by soft soil character with a fairly thick sediment thickness.

Acknowledgments. The researchers would like to thank all the people who are involved in this research for their valuable contribution and cooperation in conducting this research.

Authors' Contributions. This research data is collected and analyzed by Siti Rohmah and Farizky Hisyam. Then, Mr. Adi Susilo was a corresponding author. Then, Mr. Eko Andi Suryo, Mr. Sarijan, and Mr. Sarjiyana as advisors and consultants.

References

1. K. Lilik, R. Yunus, robi amir Muhammd, and P. Narwawi, "Indek Kerawanan Bencana Indonesia," pp. 1–226, 2011.
2. P. Purbandini, B. J. Santosa, and B. Sunardi, "Analisis Bahaya Kegempaan di Wilayah Malang Menggunakan Pendekatan Probabilistik," *J. Sains dan Seni ITS*, vol. 6, no. 2, 2017, doi: <https://doi.org/10.12962/j23373520.v6i2.25221>.
3. A. Susilo and Z. Adnan, "Probabilistic Seismic Hazard Analysis of East Java Region, Indonesia," *Int. J. Comput. Electr. Eng.*, vol. 5, no. 3, pp. 341–344, 2013, doi: <https://doi.org/10.7763/ijcee.2013.v5.728>.
4. A. Koulali *et al.*, "Crustal strain partitioning and the associated earthquake hazard in the eastern Sunda-Banda Arc," *Geophys. Res. Lett.*, vol. 43, no. 5, pp. 1943–1949, 2016, doi: <https://doi.org/10.1002/2016GL067941>.
5. N. I. Desmonda and A. Pamungkas, "Penentuan Zona Kerentanan Bencana Gempa Bumi Tektonik di Kabupaten Malang Wilayah Selatan," *J. Tek. POMITS Vol. 3, No. 2*, vol. 3, no. 2, pp. 107–112, 2014.
6. V. A. Sokolov, T. K. Tarakanova, and E. A. Abdyrakhmanova, "The third international conference on apomixis," *Russ. J. Genet.*, vol. 44, no. 11, pp. 1367–1375, 2008, DOI: <https://doi.org/10.1134/S1022795408110203>.
7. N. Haerudin, F. Alami, and Rustadi, *Mikroseismik, Mikrotremor dan Microearthquake Dalam Ilmu Kebumihan*. 2019.

8. I. L. Figlio and D. Uomo, "Self, Subjectivity, And Identity—Their Antecedents, Emergent Contours And Contemporary Relevance," vol. 379, no. 1, pp. 350–379, 1971.
9. Y. Nakamura, "Nakamura_1989.pdf," *QR of RTRI*, vol. 30, p. 1, 1989.
10. P. Bard, A. Duval, A. Koehler, and S. Rao, "Guidelines for the Implementation of the H/V Spectral Ratio Technique on Ambient Vibrations Measurements, Processing, and Interpretation," *Interpret. A J. Bible Theol.*, vol. 169, no. December, pp. 1–62, 2004, DOI: <https://doi.org/10.1111/j.1365-246X.2006.03282.x>.
11. Y. Nakamura, "Clear Identification of Fundamental Idea of Nakamura 'S,'" *Spectrum*, p. 2656, 2000.
12. J. Hasil, P. Bidang, M. Seismic, and D. I. Medina, "EINSTEIN (e-Journal)," 2020.
13. A. M. Arifudin, "Karakteristik Situs dan Kerentanan seismik di kabupaten Klaten dengan Metode Horizontal to Vertical Spectral Ratio (HVSr) dari Data Mikrotremor," p. 146, 2018.
14. R. Tuladhar, F. Yamazaki, P. Warnitchai, and J. Saita, "Seismic microzonation of the greater Bangkok area using microtremor observations," *Earthq. Eng. Struct. Dyn.*, vol. 33, no. 2, pp. 211–225, 2004, DOI: <https://doi.org/10.1002/eqe.345>.
15. D. Karnawati, "the Mechanism of Rock Mass Movements As the Impact of Earthquake ;" *Din. Tek. Sipil*, vol. 7, no. 1979, pp. 179–190, 2007.
16. Marjiyono, Ratdomopurbo, Suharna, H. M. H. Zajuli, and R. Setianegara, "Geologi bawah permukaan dataran klaten berdasarkan interpretasi data mikrotremor," vol. 15, no. 1, pp. 3–10, 2014.
17. Y. Nakamura, "On the H/V spectrum," *14th World Conf. Earthq. Eng.*, pp. 1–10, 2008, [Online]. Available: http://117.120.50.114/papers/14wcee/14wcee_hv.pdf

Open Access This chapter is licensed under the terms of the Creative Commons Attribution-NonCommercial 4.0 International License (<http://creativecommons.org/licenses/by-nc/4.0/>), which permits any noncommercial use, sharing, adaptation, distribution and reproduction in any medium or format, as long as you give appropriate credit to the original author(s) and the source, provide a link to the Creative Commons license and indicate if changes were made.

The images or other third party material in this chapter are included in the chapter's Creative Commons license, unless indicated otherwise in a credit line to the material. If material is not included in the chapter's Creative Commons license and your intended use is not permitted by statutory regulation or exceeds the permitted use, you will need to obtain permission directly from the copyright holder.

